Journal of Catalysis 262 (2009) 1–8

Contents lists available at ScienceDirect

Journal of Catalysis

www.elsevier.com/locate/jcat

FAPO and Fe-TUD-1: Promising catalysts for N_2O mediated selective oxidation of propane?

Wei Wei, Jacob A. Moulijn, Guido Mul *

Catalysis Engineering, DelftChemTech, Delft University of Technology, Julianalaan 136, 2628 BL Delft, The Netherlands

ARTICLE INFO

Article history:
Received 7 June 2008
Revised 18 November 2008
Accepted 21 November 2008
Available online 24 December 2008

Keywords:
$AlPO_4$-5
TUD-1
Iron
Fe
FAPO
N_2O
Propane
Selective oxidation
Deactivation
Operando DRIFT
Infrared
Carboxylates

ABSTRACT

Iron (2 wt%) was incorporated into the structure of microporous $AlPO_4$-5 (FAPOcal) and the mesoporous materials TUD-1 and Al-TUD-1 (Fe-TUD-1 and Fe-Al-TUD-1). FAPOcal was also additionally modified by steaming (FAPOste). Compared to literature data on optimized Fe-ZSM-5, FAPOcal shows relatively low activity and comparable selectivities in N_2O induced propane selective oxidation. Steaming reduces the performance of this $AlPO_4$-5 based catalyst. Fe-TUD-1 and Fe-Al-TUD-1 are less active and selective than FAPOcal. However, the stability of the investigated systems is significantly better than reported for Fe-ZSM-5. This is explained by differences in surface chemistry: *operando* DRIFT studies show formation of carbonates and carboxylates on the surfaces of the FAPO and TUD-1 based catalysts, rather than coke. Reasons for the different behavior of the herein investigated catalysts as compared to Fe-ZSM-5 are discussed.

1. Introduction

Oxidative dehydrogenation of propane (ODHP) with dioxygen to produce propene has been intensively studied in the literature [1–3]. A problem of this route is extensive CO_x formation already at moderate conversions, leading to low propene selectivity. N_2O is an attractive alternative oxidation agent for ODHP, steam-activated Fe-ZSM-5 being a promising catalytic system showing high initial activity and selectivity to propene. The activity and selectivity are comparable with those reported for V- and Mo-based catalysts, employing dioxygen [4,5]. Unfortunately, a major drawback of iron zeolites in ODHP with N_2O is deactivation by coke, causing a rapid decrease of the propylene yield [6].

Another promising catalytic system reported in the literature for the application of N_2O-mediated oxidation is bulk $FePO_4$. When N_2O or mixtures of H_2 and O_2 are used as oxidants [7,8], this catalyst shows low activity but remarkable selectivity in oxidation of light alkanes to alcohols (C_1–C_2), assigned to a selectivity promoting function of the phosphate groups. A way to potentially combine the high activity of iron sites in a zeolite matrix with the functionality of the phosphate groups is the use of iron-incorporated aluminophosphate molecular sieves Fe-$AlPO_4$-5 (FAPO). While these sieves are hardly active in direct N_2O decomposition, even after steaming [9], they show comparable activity to Fe-ZSM-5 in the conversion of benzene to phenol [10]. The activity of iron-incorporated aluminophosphate molecular sieves in N_2O mediated propane ODH has not been previously investigated.

The aim of the present paper is to evaluate the activity, selectivity and stability of FAPO, before and after steaming, in the N_2O-mediated ODHP reaction. To evaluate the nature of the active site, as well as to assess the role of the pore structure, the catalytic performance of FAPO is compared with Fe-TUD-1 and aluminum promoted Fe-TUD-1 [11,12]. In particular the nature of deposits formed on the catalyst surfaces during the reaction is analyzed by DRIFT spectroscopy, and discussed in relation to the observed deactivation behavior.

2. Experimental

2.1. Catalyst synthesis procedures

An iron substituted $AlPO_4$-5 catalyst was synthesized according to the recipe of Catana et al. [13]. An iron source (Fe^{3+} chloride hexahydrate; Janssen Chimica) was added to a solution of

* Corresponding author.
E-mail address: g.mul@tudelft.nl (G. Mul).

0021-9517/$ – see front matter
doi:10.1016/j.jcat.2008.11.015

phosphoric acid (85 wt% solution in water; Janssen Chimica) and water while stirring, until complete dissolution. Pseudo-boehmite (Catapal; 70% Al_2O_3, 30% H_2O; Vista) was added under vigorous stirring, followed by the dropwise addition of triethylamine (TEA 99%; Janssen Chimica). All reagents were mixed in an ice bath. The obtained gel with a molar composition 1.0 TEAOH:0.004 Fe:0.996 Al:1.0 PO_4:80 H_2O was stirred for 1 h and heated in a Teflon-lined autoclave at 150 °C for 20 h. The resulting solid was washed and then dried at 60 °C. Then it was calcined at 500 °C in static air for 10 h applying a ramp rate of 5 °C/min in air to remove the template (denoted as 2FAPOcal). Afterward, a fraction (500 mg) of the powdered sample was steamed in a quartz reactor with a 30 ml(STP) min^{-1} flow containing a water partial pressure of 300 mbar in N_2 at 600 °C for 5 h, again applying a ramp rate of 5 °C/min to heat the sample from room temperature to 600 °C. The sample is denoted as 2FAPOste.

Tetraethylorthosilicate (TEOS, +98% ACROS), triethanolamine (TEA, 97%, ACROS), tetraethyl ammonium hydroxide (TEAOH, 35% Aldrich) and the iron source ferric chloride ($FeCl_3$, Aldrich) were used for the synthesis of the Fe-TUD-1 mesoporous material [11,12,14]. A mixture of 25 g TEA and 18.4 mL of de-ionized water was added drop-wise into a mixture of 34.6 g TEOS and 1.33 g $FeCl_3$, while stirring vigorously. After stirring for about 30 min, 20.5 g of TEAOH was added. The mixture was aged at room temperature for 24 h, dried at about 100 °C for 24 h and then hydrothermally treated in a Teflon-lined stainless steel autoclave at 180 °C for 8 h. Finally the solid, as-synthesized samples were calcined at 600 °C for 10 h using a ramp rate of 1 °C/min in air (denoted as 2Fe-TUD-1).

For bi-metallic 2Fe-2Al-TUD-1, 1.23 g aluminum isopropoxide (Aldrich) was used as alumina source and added together with the $FeCl_3$ solution. The remainder of the procedure is the same as described above, involving aging, hydrothermal treating and calcination of the homogeneous synthesis mixture.

2.2. Characterization techniques

The amount of P in the chemical composition of the catalysts was determined by ICP-OES (Perkin Elmer Optima 4300DV). The elemental analysis of the other elements, i.e. Fe, and Al was determined using instrumental neutron activation analysis (INAA), conducted on a THER nuclear reactor with a thermal power of 2 MW and maximum neutron reflux of 2.10 $m^{-2}\,s^{-1}$. The method proceeds in three steps: irradiation of the elements with neutrons in the nuclear reactor, followed by a period of decay, and finally a measurement of the radioactivity resulting from irradiation. The energy of the radiation and the half-life period of the radioactivity enable a highly accurate quantitative analysis.

Nitrogen ad- and desorption isotherms were recorded at −196 °C on a QuantaChrome Autosorb-6B. Prior to the analysis, the samples were evacuated and preheated at 300 °C overnight. The BET method was used to calculate the surface area (S_{BET}), and the total pore volume (V_{tot}) was obtained at 0.99 p/p_0. The pore size distribution was calculated from the adsorption branch using the Barret–Joyner–Halenda (BJH) model, while the *t*-plot method was used to calculate the pore volume (V_{micro}). For FAPO catalysts, Ar adsorption isotherms at −184 °C were obtained in a Micromeritics ASAP 2010 apparatus. The pore size distribution was calculated from the adsorption branch of the isotherm using the Satio–Foley (SF) model.

Transmission electron microscopy (TEM) was performed using a Philips CM30T electron microscope with a LaB6 filament as the source of electrons, and a Phillips CM30UT electron microscope with a FEG as source of electrons, both operated at 300 kV. Samples were mounted on a Quantifoil® microgrid carbon polymer, supported on a copper grid from an ethanol suspension.

Fourier transform infrared (FTIR) was carried out in a Nicolet Magna 550 Fourier transform spectrometer, equipped with a high-temperature cell, in which the as-synthesized, calcined and steamed samples were placed in a holder. To characterize the Fe-sites in the obtained materials by NO adsorption, diffuse reflectance infrared Fourier transformed (DRIFT) spectra were recorded in a flow of 30 ml/min, 5 vol% NO in He at 100 °C. The spectra were acquired by coaddition of 256 scans with a nominal resolution of 4 cm^{-1}. Using the same DRIFT accessory, which was coupled to a mass spectrometer, the ODHP reaction was analyzed. The feed composition in these experiments was 0.5 vol% propane and 1.0 vol% N_2O with He as balance gas. The IR-MS system has been described in detail elsewhere [15].

2.3. N_2O-induced propane ODH

The N_2O-induced propane oxidative dehydrogenation was carried out in a six-flow reactor set-up. The set up, and definitions applied for conversion, selectivity, and yield were described in detail elsewhere [16]. The turnover frequencies (TOF) were calculated by assuming all Fe in the catalysts to participate in the reaction. In other words, the TOF is defined as the number of moles of N_2O (or propane) converted per second ($n_{react.convert.}$) per mole of iron in the catalyst ($n_{Fe\text{-}present}$), using the following formula:

$$\mathrm{TOF} = \frac{n_{\mathrm{react.convert.}}\ (\mathrm{mole})}{n_{\mathrm{Fe\text{-}present}}\ (\mathrm{mole})}\ (\mathrm{s}^{-1}).$$

The catalysts were ground and sieved to a size of 150–212 μm. Before reaction, 50 mg of all the samples was pre-treated in 50 ml/min He at 400 °C for 1 h. This was followed by increasing the temperature to 500 °C, and switching the feed to 50 ml/min 1% N_2O in He. All samples show hardly activity in N_2O decomposition, as discussed previously [9]. Then the samples were cooled down to 375 °C, and the reaction mixture was changed to 50 ml/min 1% N_2O and 0.5% C_3H_8. It should be mentioned that an excess of N_2O in the ODHP was used to limit coke formation, while studies reported in the literature typically used a N_2O/C_3H_8 ratio of one at significantly higher propane feed concentrations [5]. This was followed by increasing the temperature with a rate of 10 °C/min to 525 °C, at which steady state performance was determined.

C_3H_8, C_3H_6, O_2, CO, CO_2 and H_2O were analyzed with a GC (Chrompack CP9001) equipped with a thermal conductivity detector (TCD) and a flame ionization detector (FID), using a Poraplot Q column (for C_3H_8, C_3H_6, CO_2 and H_2O separation) and a Molsieve 5 Å column (for O_2 and CO separation). Each GC measurement was performed after a stabilization time of at least 20 min.

3. Results

3.1. Characterization – composition and morphology

The elemental composition and characterization data of all the samples are summarized in Table 1. The N_2 and Ar adsorption isotherms have been discussed and presented elsewhere [9,11,12]. The micropore size distribution of the 2FAPOcal maximizes at 0.64 nm, which is characteristic of the $AlPO_4$-5 structure. After steaming, the micropore volume and surface area are significantly reduced, suggesting that a fraction of the micropores are blocked or have collapsed as a result of the steaming procedure [9]. The steam treatment did not result in new phases, while the long-range structural order of $AlPO_4$-5 was basically maintained, as evident from XRD data reported elsewhere [9].

N_2 sorption isotherms of 2Fe-TUD-1 indicate a pore volume of 1.24 cm^3/g, and a relatively narrow pore size distribution maximizing at approximately 11.5 nm. HR-TEM analysis confirmed that 2Fe-TUD-1 consists of the sponge-like structure of TUD-1 with no

Table 1
The results of elemental analysis and N_2 sorption on 2FAPOcal, 2FAPOste, 2Fe-TUD-1, 2Fe-2Al-TUD and 3Al-TUD-1.

Sample code	Fe (wt%)	Al (wt%)	P (wt%)	S_{BET} (m^2/g)	V_{total} (cm^3/g)	d_p (nm)
2FAPOcal	2.0	21.4	25	254	0.16	0.64
2FAPOste	2.1	21.5	25	128	0.11	0.65
2Fe-TUD-1	2.0	–	–	625	1.24	11.5
2Fe-2Al-TUD-1	2.0	2.0	–	710	0.57	3.4
3Al-TUD-1	–	3.0	–	726	0.62	3.7

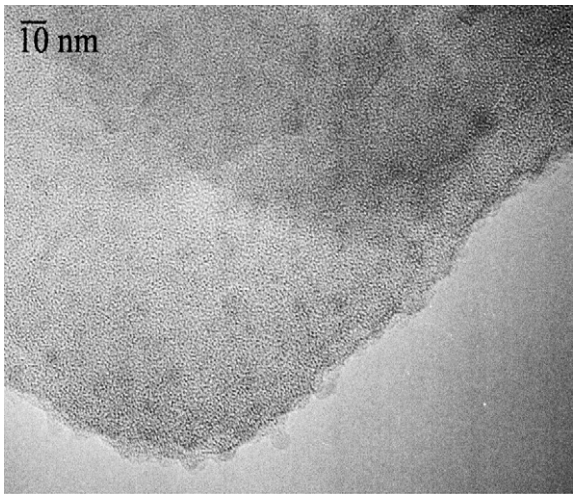

Fig. 1. TEM micrograph of 2Fe-2Al-TUD-1.

particles evident (comparable to 1Fe-TUD-1 as presented in [12]). For 2Fe-2Al-TUD-1, the pore volume is 0.55 cm^3/g and the pore size distribution maximizes at only 3.4 nm. The low pore volume and small pore size of 2Fe-2Al-TUD-1 is comparable to the characteristics of 3Al-TUD-1 [14]. This suggests that Al is not very well dispersed on the walls of the SiO_2 based channels in the preparation procedures. Instead, particles composed of Al and/or Fe-Al oxides might exist, affecting apparent pore volume and sizes. This is confirmed by the HR-TEM image of 2Fe-2Al-TUD-1 (Fig. 1), which shows the presence of particles in a size range of ~10 nm. The morphology is comparable to other TUD-1 formulations with approximately 5 wt% metal oxide loading, as discussed elsewhere [11,12]. XRD analysis suggests that both 2Fe-TUD-1 and 2Fe-2Al-TUD-1 are non-crystalline, meso-structured materials (not shown for brevity). Apparently, the particles observed in the TEM pictures of 2Fe-2Al-TUD-1 are amorphous in nature, or too low in concentration to be detected in a X-ray diffractogram.

3.2. Characterization – nature of the Fe-sites

To characterize the nature of the Fe-sites in the four catalytic materials, IR spectroscopy of adsorbed NO was performed. The results are shown in Fig. 2. An NO absorption feature at 1830 cm^{-1}, tentatively assigned to NO adsorbed on ex-framework Fe^{2+}-sites [17], is apparent in the spectrum of 2FAPOste. This band is hardly visible in the spectrum of 2FAPOcal [9]. This suggests a larger quantity of Fe^{2+} sites to be formed upon steaming, in agreement with the results of other characterization techniques. After steaming, migration of Fe from tetrahedral positions to octahedral positions has also been identified by increasing UV–Vis absorptions at wavelengths larger than 350 nm [9]. The migration of Fe to ex-framework positions induced by steaming is well known for Fe-ZSM-5 catalysts [18].

Fig. 2 also shows the absorption features of adsorbed NO on the surfaces of 2Fe-TUD-1 and 2Fe-2Al-TUD-1. NO adsorption on mesoporous 2Fe-TUD-1 is very weak and hard to detect in the FTIR measurements, suggesting that little Fe^{2+} sites are present or accessible to NO. In contrast, NO adsorbs strongly on the surface of 2Fe-2Al-TUD-1, and two peaks at 1874 and 2151 cm^{-1} are readily identified. These two peaks were previously reported in [17,19] for steam-activated ex-Fe-ZSM-5: the peak at 2133 cm^{-1} was assigned to NO adsorbed on cationic sites associated with Al^{3+} in the zeolite structure, and the peak at 1874 cm^{-1} to Fe^{2+} at extra-framework positions.

We previously proposed the presence of mixed Fe–Al oxide nanoparticles to contribute to the spectral signature of adsorbed NO in Fe-ZSM-5, and propose similar species to be present on the amorphous silica matrix of TUD-1. This is supported by the similarity in the TEM pictures of 2Fe-2Al-TUD-1 and ex-Fe-ZSM-5 [20], and the nature of the UV–Vis spectra of 2Fe-TUD-1 and 2Fe-2Al-TUD-1 [12]. In the UV–Vis spectrum of 2Fe-2Al-TUD-1, a peak around 465 nm was detected, indicative of a significant fraction of iron oxide containing particles [12].

3.3. Catalytic performance

3.3.1. N_2O-induced propane ODH

The catalytic performance of the catalysts was evaluated in N_2O-induced propane oxidation. Fig. 3 shows the turnover frequency of N_2O and C_3H_8, and the yield to propene as a function of temperature. Since N_2O is hardly converted in the absence of propane over these catalysts [9,11], it is apparent that N_2O conversion is improved significantly due to the presence of propane in the feed. Table 2 gives the TOF and product selectivity for the catalysts at 525 °C. Around 80%, 83%, 58%, and 59% of N_2O is converted at 525 °C over 2FAPOcal, 2FAPOste, 2Fe-TUD-1, and 2Fe-2Al-TUD-1, respectively. For the FAPO catalysts, propene is the main product with a selectivity ranging from 27 to 30% at around 44% conversion, while CO and CO_2 are the main by-products and ~3% is converted to the oxygenate acrolein. 2FAPOste shows lower selectivity to propene than 2FAPOcal. Selectivity to propene is apparently not favored by extracting Fe species from the framework of 2FAPOcal. Although the applied feed conditions were different, it is evident that the FAPO systems are less active than optimized Fe-ZSM-5, comparing the TOF values reported in [5].

The propane conversion obtained for mesoporous 2Fe-TUD-1 at 525 °C is significantly lower than obtained for microporous 2FAPOcal, while at these lower conversion levels the selectivity to propene is also significantly lower. 2Fe-TUD-1 and 2Fe-2Al-TUD-1 are thus inferior catalysts to the FAPO based systems for propene production.

While the performance remains lower than reported for optimized Fe-ZSM-5 [5], it should be mentioned that the stability of the TUD-1 and FAPO based catalysts is quite good: at most a reduction in propene yield of ~3% was observed after 12 h on stream (not shown for brevity), compared to a reported drop in propane conversion from 48% to 10% after 7 h on stream for Fe-ZSM-5 [5].

It is clear from Table 2 that the C and O mass balance of the analyses of the catalysts are not closed to 100%. Besides being related to experimental errors, this suggests that oxygenates might be accumulating on the surface of the catalysts, as will be demonstrated by the investigation of the nature and extent of deposits formed on the catalyst surface during the reaction by DRIFT spectroscopy.

Fig. 4 shows the spectral development in the region where absorptions of the OH-groups of the 2FAPOcal catalyst are to be expected. The strongest intensity at 3665 cm^{-1} has been assigned to Brönsted sites, i.e. P–OH [20–23]. The weak features at 3780 cm^{-1} and ~3400 cm^{-1} are most likely associated with Al–OH [24] and hydrogen bonded OH-groups, respectively. Al–OH vibrations have been reported for mixed Ga_2O_3/Al_2O_3 catalysts [24]. Clearly, the

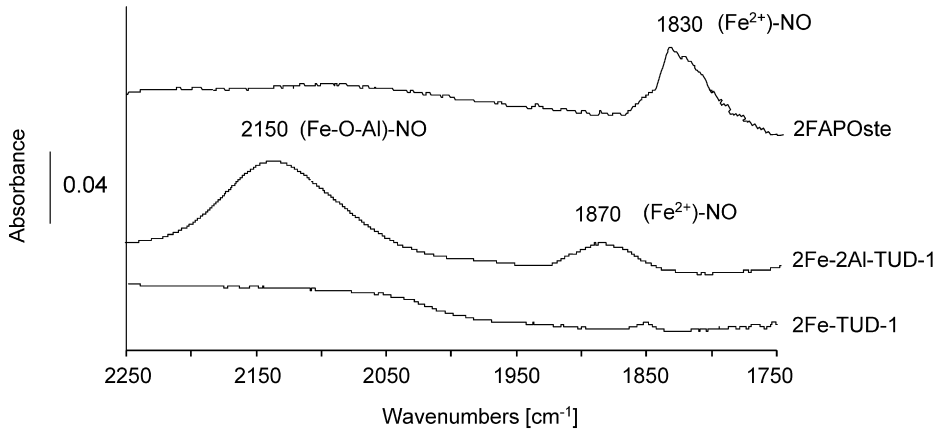

Fig. 2. Infrared spectra of NO adsorbed on 2Fe-TUD-1, 2FAPOste and 2Fe-2Al-TUD-1 at 100 °C in flow (30 ml/min) of 5 vol% NO in He against a background of the catalysts at the same temperature in He.

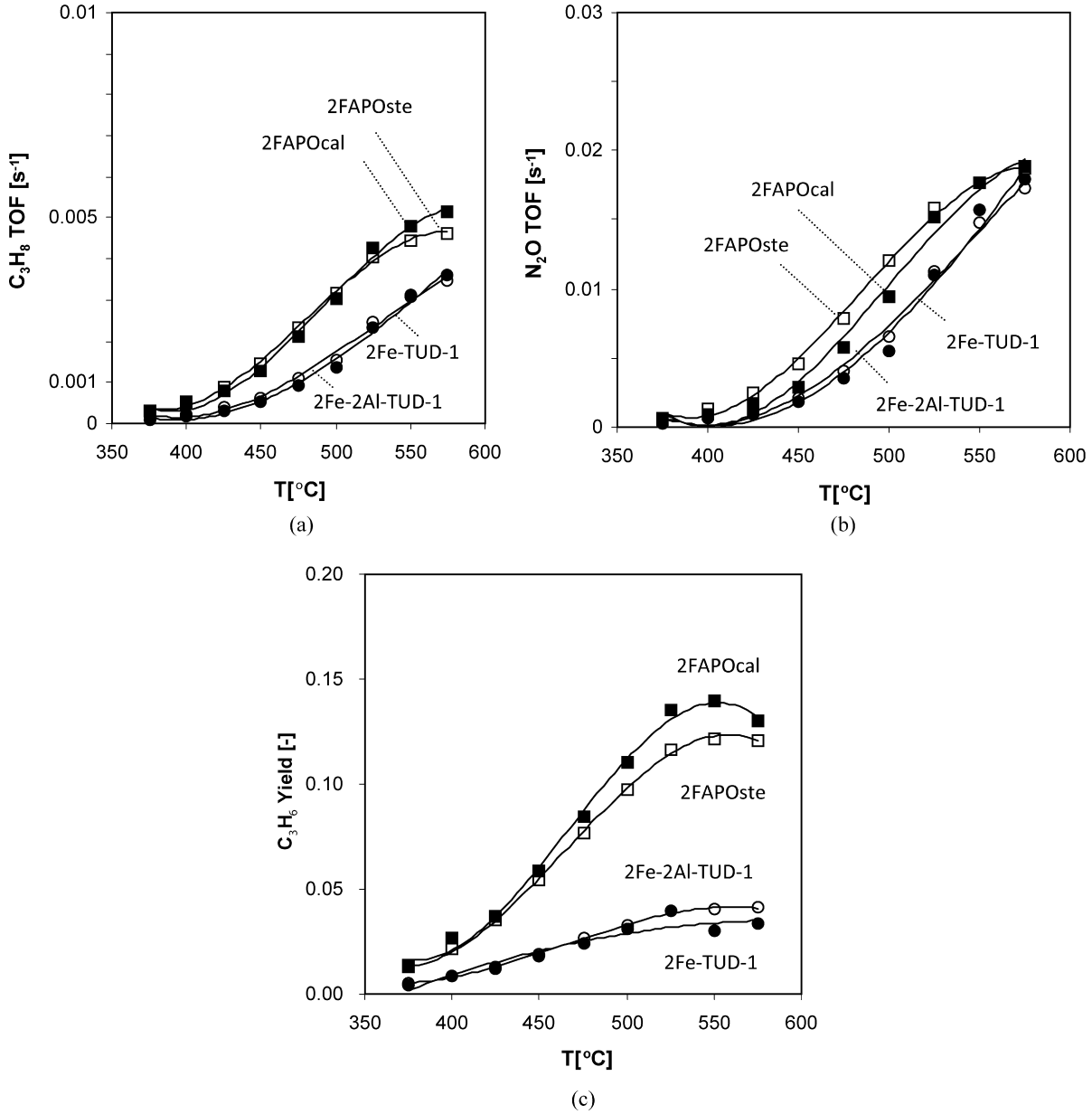

Fig. 3. N_2O, C_3H_8 TOF, and C_3H_6 yield at different temperatures over 2FAPOcal, 2FAPOste, 2Fe-TUD-1, and 2Fe-2Al-TUD-1. Feed conditions: C_3H_8:N_2O:He = 1:2:97; $P = 1$ bar.

Table 2
The TOF of propane and nitrous oxide and the selectivity to propene, carbon monoxide, carbon dioxide and acrolein. Reaction conditions: C_3H_8:N_2O:He = 1:2:197; $P = 1$ bar; $T = 525\,^{\circ}C$.

	TOF (s^{-1})		Selectivity (%)				Element balance (%)	
	C_3H_8	N_2O	C_3H_6	CO	CO_2	Acrolein	C	O
2FAPOcal	0.0043	0.0152	30	12	32	3	77	64
2FAPOste	0.0041	0.0158	27	13	39	2	82	71
2Fe-TUD-1	0.0023	0.0110	16	23	47	2	88	74
2Fe-2Al-TUD-1	0.0025	0.0113	15	22	45	1	82	73

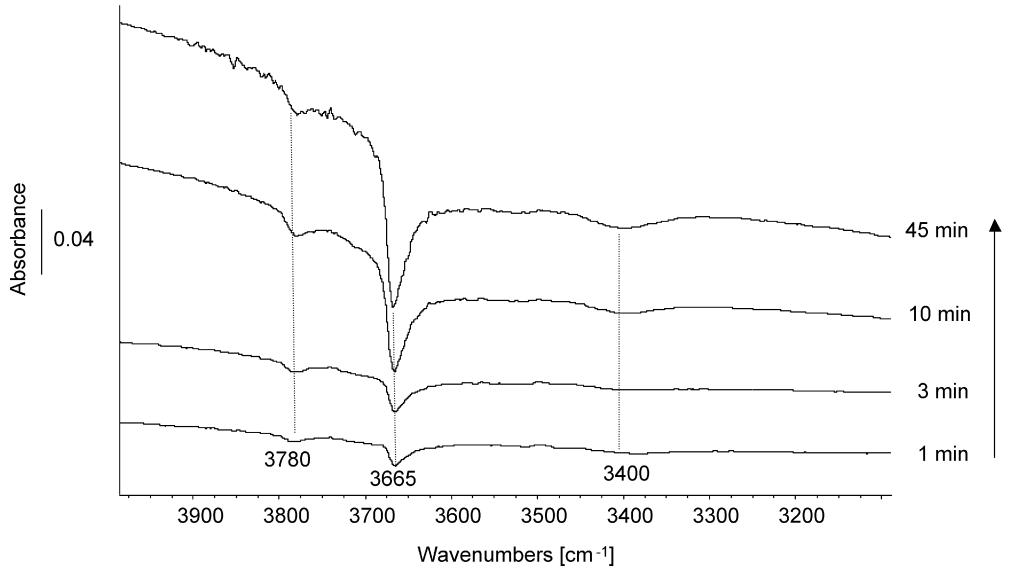

Fig. 4. Development of infrared spectra in the region of 3000–4000 cm^{-1} for 2FAPOcal against a background of the catalysts at the same temperature in He. Feed conditions: C_3H_8:N_2O:He = 1:2:197; $P = 1$ bar; $T = 525\,^{\circ}C$.

negative intensities of the OH related features at 3780, 3665, and 3400 cm^{-1} intensify, suggesting that OH-groups are converted by interaction with products of propane oxidation.

Certainly features in the 1200 to 1800 cm^{-1} region of the spectra indicate the formation of strongly bound surface adsorbed species (see Fig. 5). The most predominant bands in the region 1400–1650 cm^{-1} have been assigned to carboxylate and carbonate type species on the surface of various support materials [24,25]. The band at ~1585 cm^{-1} has typically been assigned to formate [24,26], while the lower band frequencies are most likely related to acetate vibrations (ν_{as}(COO), 1564 cm^{-1}, ν_s(COO), ~1450 cm^{-1}). The band observed in the later stages of the reaction at ~1720 cm^{-1}, is most likely related to adsorbed acrolein, in view of the product distribution observed in the gas phase analyses. The strong band at ~1300 cm^{-1} has not been previously reported in the literature on propane oxidation over metal oxide catalysts. Frei and coworkers adsorbed acetaldehyde on FAPO [22], with the C–H bending modes located in the region 1350–1400 cm^{-1}, rather than at 1300 cm^{-1}. Only bands in the 1350–1400 cm^{-1} region were observed after formic acid or acetic acid adsorption on alumina surfaces, whereas acrolein adsorption does not give rise to the low frequency band at 1300 cm^{-1} either. Two options remain: nitrate bands have been assigned to absorptions in the region of 1290–1310 cm^{-1}. If nitrates are formed, this is most likely the result of a small fraction of NO in the N_2O feed applied, which is commonly the case. Alternatively, the band might be related to phosphate vibrational modes, which are enhanced by the changes in the chemical environment of the phosphate groups upon deposition of the carbonates and carboxylates.

In the experiment conducted with 2FAPOste, the IR bands are located at similar positions (not shown for brevity) as observed for 2FAPOcal, besides the presence of an additional band, located at 3735 cm^{-1}. The novel band at 3735 cm^{-1} is most likely related to ex-framework Al species, in view of literature assignments [24]. In the 1200 to 1800 cm^{-1} region the bands are also quite similar before and after steaming, indicating that the surface species formed on the steamed and calcined FAPO are alike. It should be mentioned that both catalysts turned black during the *in situ* analysis, suggesting that besides the carboxylates, some carbon is deposited on the surface of the catalysts, which does not have an IR signature. After flushing the DRIFT cell with He, we were unable to identify the C–H stretches reported in a spectroscopic study on Fe-ZSM-5 catalyzed N_2O mediated ODHP [6]. We tried to analyze the samples with Raman spectroscopy to identify the aliphatic and aromatic content of the samples, but failed due to strong fluorescence of the samples at the applied laser wavelength (514 nm).

In Fig. 6, the development of the IR bands upon N_2O induced propane oxidation as a function of time is shown for the 2Fe-TUD-1 sample. Maxima of the IR absorptions are located at 1645, 1530, and 1450 cm^{-1}. In view of the product distribution, oxygenates are likely to be the surface species causing these vibrations. The broad features at 1530 and 1450 cm^{-1} are the result of acetate deposits, while the band at 1645 cm^{-1} is located in the region of hydrogen bonded carbonates (bicarbonate). The broad negative band in the 3100 to 3900 cm^{-1} region (see insert) is decreasing as a result of chemical interactions of surface OH groups with the products of propane oxidation.

4. Discussion

4.1. FAPO or Fe-TUD-1: promising catalyst formulations?

The most promising zeolitic system reported so far for N_2O mediated ODHP is steam-activated Fe-ZSM-5, displaying initial

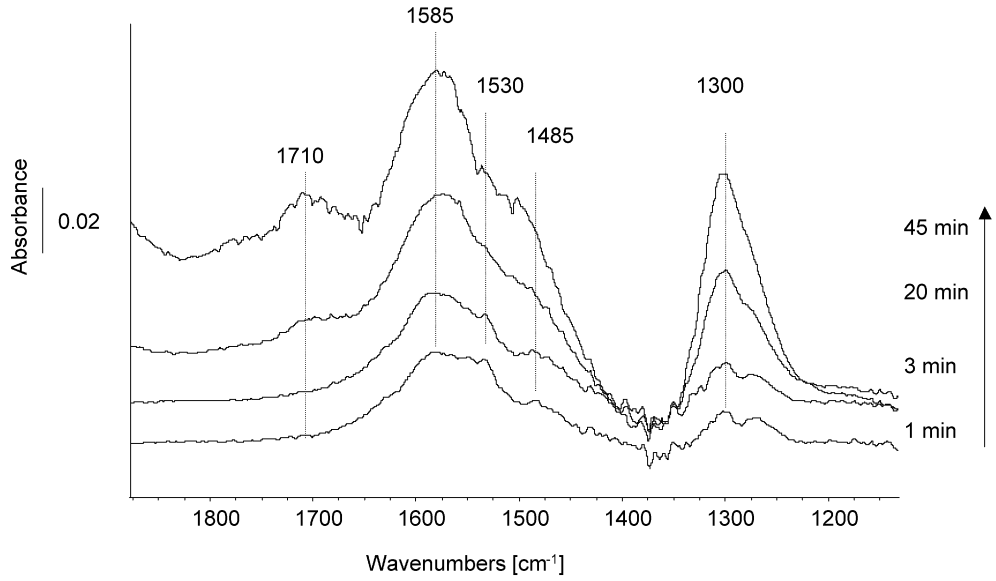

Fig. 5. Development of infrared spectra in the region of 1200–1800 cm^{-1} over 2FAPOcal against a background of the catalyst at the same temperature in He. Feed conditions: C_3H_8:N_2O:He = 1:2:197; $P = 1$ bar; $T = 525\,^{\circ}C$.

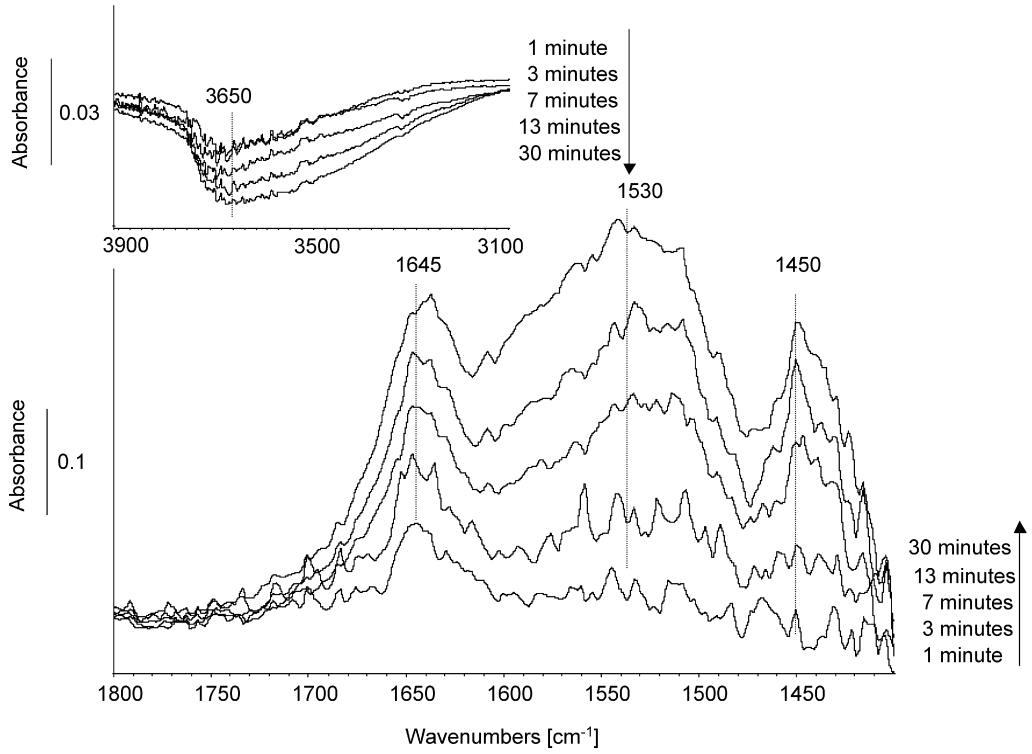

Fig. 6. Development of infrared spectra in the region of 1400–1800 cm^{-1} over 2Fe-TUD-1cal against a background of the catalyst at the same temperature in He. Insert: Development of infrared spectra in the region of 3100–3900 cm^{-1}. Feed conditions: C_3H_8:N_2O:He = 1:2:197; $P = 1$ bar; $T = 525\,^{\circ}C$.

propene yields up to 25% [4,5]. The performance of 2FAPOcal reported in the present study is significantly smaller, although the catalyst exhibits relatively high selectivity to propene. Metal phosphate catalysts generally show relatively low activity and high selectivity in oxidation reactions, such as bulk $FePO_4$ in oxidation of light alkanes to alcohols (C1–C2) [27], $Mn_2P_2O_7$ in propane oxidation to acetaldehyde, acrolein, or methanol [28], and $(VO)_2P_2O_7$ in oxidation of *n*-butane to maleic anhydride [29]. As evident from Table 2, contrary to Fe-ZSM-5, steaming does not dramatically improve the performance of 2FAPOcal: the conversion is slightly decreased, as is the selectivity to propene. Apparently the significant activity of FAPO in the N_2O mediated conversion of benzene to phenol [10] is not achieved in the conversion of propane under the applied process conditions in the present study.

Mesoporous catalysts, 2Fe-TUD-1 and 2Fe-2Al-TUD-1 show less activity and lower selectivity than the microporous FAPO catalysts. Recently Bruckner and coworkers [30] investigated the performance of mesoporous Fe-SBA-15 in the same reaction and attributed the bad performance to the low degree of adsorption of reactants, a result of the large pore size. Besides this explanation, we believe that the presence of a considerable amount of iron oxide clusters in the mesoporous 2Fe-TUD-1 and 2Fe-2Al-TUD-1, i.e.

a low dispersion, correlates with low activity. These clusters were identified to be present by UV–Vis spectroscopy and TEM images, to the largest extent in the 2Fe-2Al-TUD-1 system.

In conclusion, nor the presence of phosphate groups, nor the open pore texture of mesoporous materials, leading to relatively large FeO_x containing clusters, are beneficial for N_2O mediated ODHP. The reason for the lower activity of 2FAPOste and the 2Fe-TUD-1 and 2Fe-2Al-TUD-1 catalysts, as compared to steam-activated Fe-ZSM-5, will be further discussed in the following paragraph, on the basis of a mechanistic evaluation.

4.2. Mechanistic considerations

Activation of N_2O over Fe-ZSM-5 catalysts is generally accepted to produce α-oxygen and N_2. It has furthermore been demonstrated by the temporal analysis of products (TAP) that the recombination and desorption of α-oxygen, yielding O_2, is the rate determining step in direct N_2O decomposition over ex-Fe-ZSM-5 [17]. In view of the previously reported very low activity over FAPO in direct N_2O decomposition, this step is considered to be hardly possible over calcined FAPO, tentatively explained by the nature of Fe^{3+} sites and the vicinity of phosphate groups, which might inhibit the oxygen desorption and the regeneration of the iron sites [9]. The enhanced N_2O decomposition rate of 2FAPOcal in N_2O-mediated propane ODH is therefore very likely the result of reaction of propane with surface activated oxygen, regenerating the active site. Similar observations were reported in N_2O mediated benzene oxidation over FAPO by Sankar and coworkers [10]. The following elemental steps are proposed to be involved in the reaction:

$$N_2O + * \rightarrow N_2 + \alpha\text{-}O*, \quad (1)$$

$$2\alpha\text{-}O* \rightarrow O_2 + 2*, \quad (2)$$

$$C_3H_8 + \alpha\text{-}O* \rightarrow C_3H_6* + H_2O, \quad (3)$$

$$C_3H_6* \rightarrow C_3H_6 + *, \quad (4)$$

$$C_3H_6* + \alpha\text{-}O* \text{ or } N_2O \rightarrow \text{carboxylates}, \quad (5)$$

$$C_3H_6* \rightarrow \text{coke}. \quad (6)$$

Obviously the reaction between α-oxygen and propane, step (3), is much faster than the recombination and desorption of α-oxygen, step (2). Two neighboring sites are needed for O_2 desorption, while reaction step (3) principally only requires one, isolated, site. As a result, the N_2O conversion is greatly enhanced due to the presence of propane in the feed. Although steam treatment creates active (clustered) Fe^{2+} sites in 2FAPOste, enhancing N_2O conversion [9], the local environment of catalytic Fe^{2+} sites is chemically different (including phosphate interactions) than obtained by steaming of isomorphously substituted Fe-ZSM-5, explaining the relatively low activity of 2FAPOste as compared to steam activated Fe-ZSM-5. It should be mentioned that the steaming procedure (time, temperature) has not been optimized for 2FAPOste, and the performance can potentially be improved by alteration of this procedure. The importance of a specific isolated site created in Fe-ZSM-5 [5] is also evident from the low performance of the TUD-1 samples in the present study. While the nature of the clustered Fe-sites in the TUD-1 samples and Fe-ZSM-5 is similar, the highly active isolated site [5] is apparently not formed in the TUD-1 based catalysts.

In the following it will be discussed why the deactivating surface species formed during the reaction are so much different in nature in 2FAPO, and the TUD-1 samples, as compared to steam activated Fe-ZSM-5.

4.3. Catalyst stability

Surface species as side products of selective propane oxidation have been observed in DRIFT spectra for both FAPO systems investigated, as well as for the TUD-1 systems. These are most likely the result of consecutive reactions of propene. Once surface propene has been formed, it has three options: (i) it can desorb, (ii) the surface complex can be converted to carboxylates by reaction with surface oxygen or N_2O, and (iii) the surface complex can form coke-like species, depositing on the catalyst' surface yielding the black color. The selectivity to propene, carboxylates and coke is determined by the relative rates of reaction steps (4), (5), and (6). The discrepancy of C and O mass balance for all catalysts presented in Table 2 is consistent with oxygenate formation and coke deposition. Based on the relatively stable baseline in the DRIFT measurements, we assume the amount of coke formed to be relatively small. This is consistent with the relatively high stability of the catalysts on stream. It should be mentioned that the applied propane concentration in our studies was relatively low, and that further stability evaluation in the presence of higher propane concentrations, and at different propane/N_2O ratio should be performed, which might affect the rates of reaction steps (5) and (6).

The small deactivation rate and formation of carboxylates, rather than coke, is also tentatively explained by the relatively slow desorption rate of surface activated oxygen from 2FAPOcal, 2FAPOste, 2Fe-TUD-1 and 2Fe-2Al-TUD-1. The high oxygen coverage results in the consecutive formation of carboxylates from propene, rather than coke, which is preferred over Fe-ZSM-5 as shown by Perez-Ramirez and coworkers [6]. We propose this to be the result of a relatively low surface oxygen coverage of Fe-ZSM-5 during the reaction, as illustrated in Scheme 1. Based on the *operando* DRIFT study, the similar surface carboxylate species on 2FAPOcal and 2FAPOste suggest they are mainly interacting with P–OH or Al–OH groups, explaining the small effect on the activity of the Fe-sites. For the TUD-1 catalysts, the broad negative feature in the OH-range of the spectrum also suggests that the majority of the carboxylates and adsorbed species involve interactions with (hydrated) silanol groups.

Although the investigated catalysts show low coke formation and relatively little deactivation, the performance still does not compete with Fe-ZSM-5. While coke is relatively easily formed on ex-Fe-ZSM-5 and leads to a drop in propane conversion from 48% to 10% after 7 h on stream [4,31], it should be mentioned that deactivation is reversible, and in practice C_3H_6 can be produced continuously in a battery of parallel reactors [32].

5. Conclusions

While less effective than steam activated Fe-ZSM-5, 2FAPOcal is found active, selective and relatively stable in N_2O induced propane ODH. Extracting Fe^{3+} species from the framework of 2FAPOcal does not favor propane conversion and reduces selectivity to propene.

Mesoporous 2Fe-TUD-1 and 2Fe-2Al-TUD-1 generally exhibit lower activity and selectivity than the FAPO systems investigated, which is related to the presence of a considerable amount of iron clusters and oxides in these catalysts. This indicates that the pore structure is less important than the chemical nature of the iron sites in selective N_2O induced propane oxidation.

The nature of the deactivating surface species formed during the reaction is quite different for the investigated FAPO and Fe-TUD-1 catalysts than reported for Fe-ZSM-5 in the literature [6]. This is tentatively explained by the surface oxygen coverage of the catalytic formulations, which is proposed to be high for FAPO and Fe-TUD-1, and relatively low for Fe-ZSM-5.

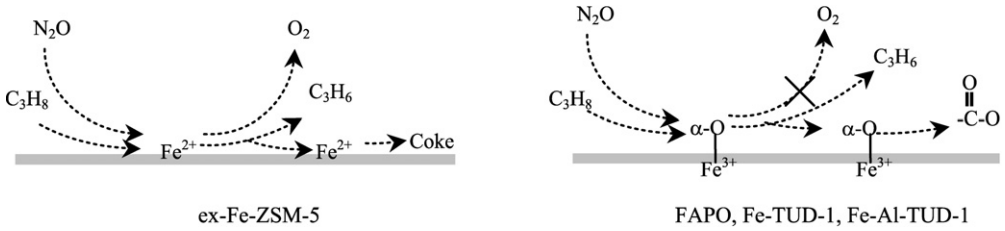

Scheme 1. Proposed reaction mechanism of N_2O induced propane oxidation on the surface of ex-Fe-ZSM-5 and FAPO, Fe-TUD-1, Fe-Al-TUD-1 catalysts.

Acknowledgments

The authors thank Mr. H. Leeman (K.U. Leuven, Belgium) and Prof. Dr. Ir. B.M. Weckhuysen (Utrecht University, the Netherlands) for providing us with FAPO-5 materials. The authors thank Dr. J.C. Groen and Drs. S. Brouwer for the gas adsorption analyses. Drs. Ing. V.C.L. Butselaar is acknowledged for the TEM experiments. Finally the National Research School Combination Catalysis, The Netherlands, is gratefully acknowledged for financial support.

References

[1] F. Cavani, N. Ballarini, A. Cericola, Catal. Today 127 (2007) 113.
[2] E.A. Mamedov, V.C. Corberan, Appl. Catal. A Gen. 127 (1995) 1.
[3] R. Grabowski, Catal. Rev. Sci. Eng. 48 (2006) 199.
[4] J. Perez-Ramirez, E.V. Kondratenko, Chem. Commun. (2006) 2152.
[5] J. Perez-Ramirez, A. Gallardo-Llamas, Appl. Catal. A Gen. 279 (2005) 117.
[6] O. Sanchez-Galofre, Y. Segura, J. Perez-Ramirez, J. Catal. 249 (2007) 123.
[7] Y. Wang, K. Otsuka, J. Catal. 171 (1997) 106.
[8] Y. Wang, K. Otsuka, J. Chem. Soc. Faraday Trans. 91 (1995) 3953.
[9] W. Wei, J.A. Moulijn, G. Mul, Micropor. Mesopor. Mater. 112 (2008) 193.
[10] N.R. Shiju, S. Fiddy, O. Sonntag, M. Stockenhuber, G. Sankar, Chem. Commun. (2006) 4955.
[11] M.S. Hamdy, G. Mul, W. Wei, R. Anand, U. Hanefeld, J.C. Jansen, J.A. Moulijn, Catal. Today 110 (2005) 264.
[12] M.S. Hamdy, G. Mul, J.C. Jansen, A. Ebaid, Z. Shan, A.R. Overweg, T. Maschmeyer, Catal. Today 100 (2005) 255.
[13] G. Catana, J. Pelgrims, R.A. Schoonheydt, Zeolites 15 (1995) 475.
[14] M.S. Hamdy, Thesis, Delft University of Technology, 2005, Chapter 2.
[15] B.A.A. Silberova, G. Mul, M. Makkee, J.A. Moulijn, J. Catal. 243 (2006) 171.
[16] J. Perez-Ramirez, R.J. Berger, G. Mul, F. Kapteijn, J.A. Moulijn, Catal. Today 60 (2000) 93.
[17] G. Mul, J. Perez-Ramirez, F. Kapteijn, J.A. Moulijn, Catal. Lett. 77 (2001) 7.
[18] J. Perez-Ramirez, F. Kapteijn, G. Mul, J.A. Moulijn, Catal. Commun. 3 (2002) 19.
[19] J. Perez-Ramirez, F. Kapteijn, G. Mul, J.A. Moulijn, J. Catal. 208 (2002) 211.
[20] P.A. Barrett, G. Sankar, C.R.A. Catlow, J.M. Thomas, J. Phys. Chem. 100 (1996) 8977.
[21] J. Jaenchen, M.J. Haanpepen, M.P.J. Peeters, J.H.M.C. van Wolput, J.P. Wolthuizen, J.H.C. van Hooff, Stud. Surf. Sci. Catal. A 84 (1994) 373.
[22] M.S. Jeong, H. Frei, J. Mol. Catal. A Chem. 156 (2000) 245.
[23] A. Ristic, N.N. Tusar, I. Arcon, N. Zabukovec Logar, F. Thibault-Starzyk, J. Czyzniewska, V. Kaucic, Chem. Mater. 15 (2003) 3643.
[24] C. He, M. Paulus, J. Find, J.A. Nickl, H.J. Eberle, J. Spengler, W. Chu, K. Koehler, J. Phys. Chem. B 109 (2005) 15906.
[25] D.J. Yates, J. Phys. Chem. 65 (1961) 746.
[26] A.R. Almeida, J.A. Moulijn, G. Mul, J. Phys. Chem. C 112 (2008) 1552.
[27] Y. Wang, K. Otsuka, J. Mol. Catal. A Chem. 111 (1996) 341.
[28] Y. Takita, H. Yamashita, K. Moritaka, Chem. Lett. (1989) 1733.
[29] H. Imai, Y. Kamiya, T. Okuhara, J. Catal. 251 (2007) 195.
[30] M.S. Kumar, J. Perez-Ramirez, M.N. Debbagh, B. Smarsly, U. Bentrup, A. Brückner, Appl. Catal. B Environ. 62 (2006) 244.
[31] J. Perez-Ramirez, A. Gallardo-Llamas, J. Catal. 223 (2004) 382.
[32] A. Gallardo-Llamas, C. Mirodatos, J. Perez-Ramirez, Ind. Eng. Chem. Res. 44 (2005) 455.